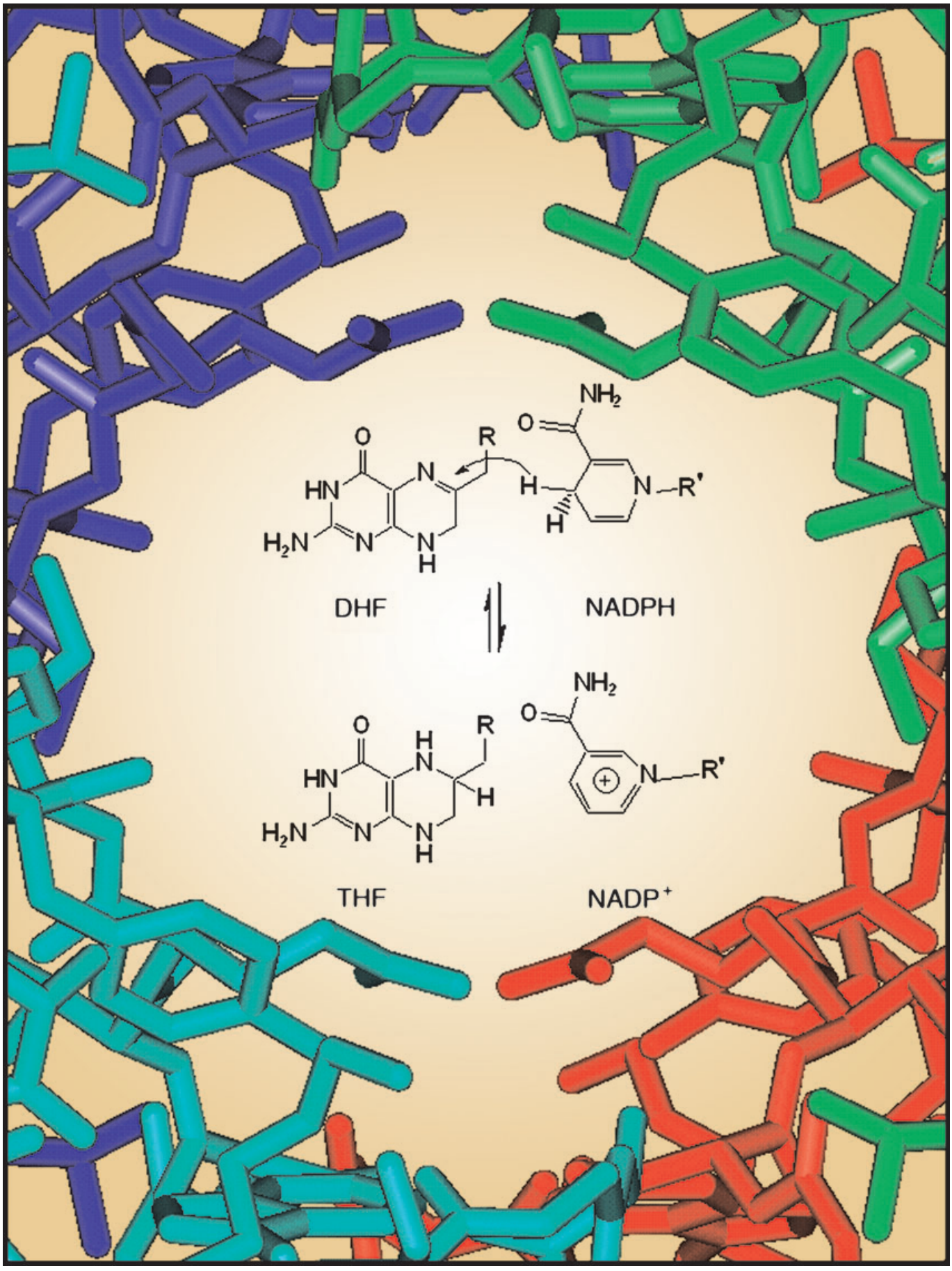

DOI: 10.1002/cbic.200400237 ChemBioChem **2005**, 6, 590 – 600

Searching Sequence Space: Two Different Approaches to Dihydrofolate Reductase Catalysis

Elizabeth E. Howell*[a]

There are numerous examples of proteins that catalyze the same reaction while possessing different structures. This review focuses on two dihydrofolate reductases (DHFRs) that have disparate structures and discusses how the catalytic strategies of these two DHFRs are driven by their respective scaffolds. The two proteins are E. coli *chromosomal DHFR (*Ec *DHFR) and a type II R-plasmid-encoded DHFR, typified by R67 DHFR. The former has been described as a very well evolved enzyme with an efficiency of 0.15, while the latter has been suggested to be a model for a "primitive" enzyme that has not yet been optimized by evolution. This comparison underlines what is important to catalysis in these two enzymes and concurrently highlights fundamental issues in enzyme catalysis.*

1. Introduction

Dihydrofolate reductase (EC 1.5.1.3) reduces dihydrofolate (DHF) to tetrahydrofolate (THF) using NADPH as a cofactor. Chromosomal DHFR is a target for inhibition by the antibacterial drug trimethoprim (TMP). Inhibition of DHFR activity by TMP leads to bacterial cell death. Clinical resistance to TMP has been observed and correlated with production of novel DHFRs that are differentially inhibited by TMP. Classification of plasmid-encoded DHFR genes indicates two families (*dfrA* and *dfrB*) with at least 17 different sequences, designated types I–XVII (see ref. [1] and references therein). Key amino acids important for substrate and cofactor binding in chromosomal DHFRs are conserved in the *dfrA* family; this suggests that they are related to chromosomal DHFR. Type II DHFR of the *dfrB* family is of particular interest as it is unrelated genetically and structurally to chromosomal DHFR. The origin of type II DHFR genes is not known, and recent Psi-BLAST searches have not yielded any clues. Some information comparing *E. coli* chromosomal DHFR and R67 DHFR, a type II DHFR, is summarized in Table 1.

Table 1. *A brief comparison of DHFRs.*

	E. coli chromosomal DHFR	R67 DHFR
enzyme form	monomer, 18 000 Da	tetramer, 34 000 Da
crystal structure	eight-stranded β sheet with four α-helical connecting strands	four β barrels, single active site pore composed of residues from four subunits
volume of active site (CASTp)[a]	1677 Å^3 (1RA2)	3626 Å^3 (tetramer from 1VIE)
trimethoprim K_i	20 pM[b]	0.15 mM[c]
dihydrofolate K_m	1.2 μM[d]	5.8 μM[e]
NADPH K_m	0.94 μM[d]	3.0 μM[e]
k_{cat} (pH 7)	29 s^{-1} (product release)[d] 240 s^{-1} (hydride transfer)[f]	1.3 s^{-1} (hydride transfer)[e]
rate-determining step	product (THF) release[g]	hydride transfer[h]

[a] Volume enclosed by active site calculated by CASTp[98] (see http://cast.engr.uic.edu/cast/). [b] From ref. [99]. [c] From ref. [100]. [d] From ref. [49]. [e] From ref. [101]. [f] From ref. [48]. [g] From ref. [21]. [h] From ref. [34].

The ability of two disparate catalytic strategies to provide DHFR activity to the cell probably arises from the reasonably simple reaction catalyzed. The basic strategy involves juxtapositioning of the substrate and cofactor, followed by protonation and hydride-transfer events.

In each section of this review, the initial focus will be on *E. coli* (*Ec*) DHFR, followed by R67 DHFR. A general comparison is given at the end of each section. Since chromosomal DHFRs have been the focus of numerous reviews,[2–7] more detail will be provided for R67 DHFR.

2. Structures

A comparison of the crystal structures for both *Ec* chromosomal and R67 DHFRs in Figure 1 A and B shows no resemblance. Chromosomal DHFRs possess an eight-stranded β-sheet core with four α helices also present.[8] The basic structure consists of two rigid subdomains separated by a hinge region.[9] The adenosine-binding subdomain binds the adenosine moiety of NADPH; the rest of NADPH, as well as folate, binds between

[a] *Prof. E. E. Howell*
Department of Biochemistry, Cellular and Molecular Biology
University of Tennessee, Knoxville, TN 37996-0840 (USA)
Fax: (+1) 865-974-6306
E-mail: lzh@utk.edu

 DOI: 10.1002/cbic.200400237

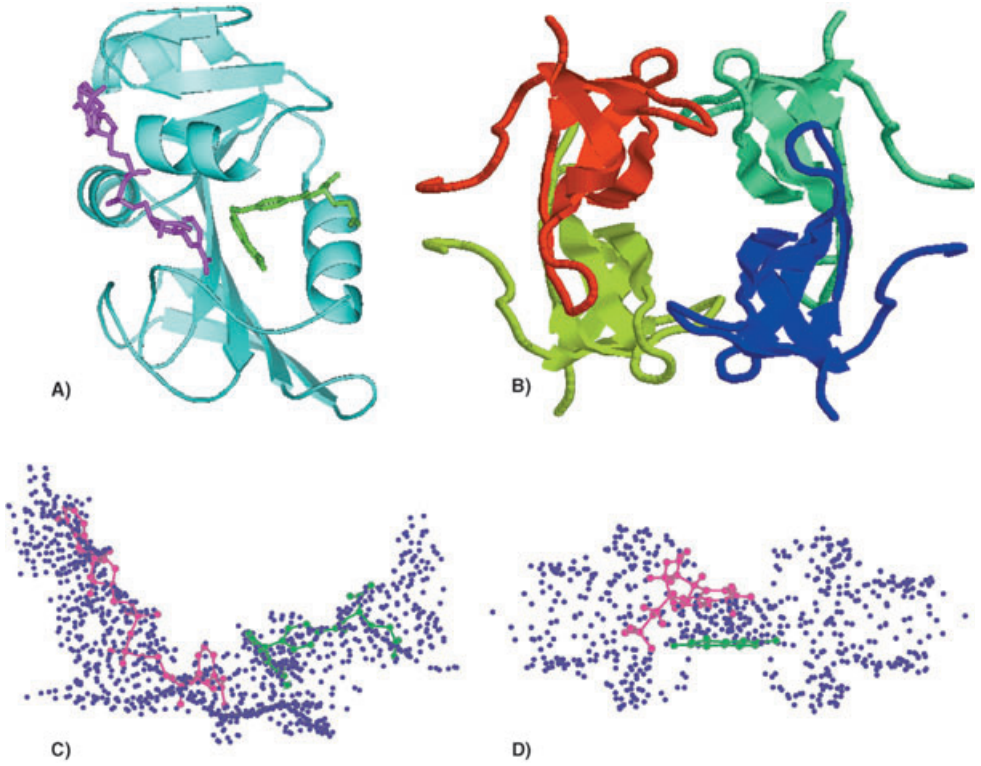

Figure 1. *Cartoon structures of A)* Ec *chromosomal DHFR and B) R67 DHFR. The positions of bound folate (green) and NADP$^+$ (magenta) are shown in the Ec DHFR structure (1A2 from the protein data bank). R67 DHFR (1VIE) is a dimer of dimers, each monomer is colored differently. The monomer–monomer interfaces occur on the sides of the structure (sea green + blue or chartreuse + red), while the dimer–dimer interfaces occur on the top and bottom of the structure (sea green + red or chartreuse + blue). The active site pore is the hole in the center. C, D) The reverse images for each active site were generated by SPHGEN, a subroutine of DOCK.[27] In the reverse images, each sphere point describes a potential atom position for use by the docking algorithm. The positions of bound folate (green) and NADP$^+$ (magenta) are shown for Ec DHFR,[20] while the positions of the pteridine ring of folate (Fol I in 1VIF) and docked NMNH are shown for R67 DHFR.[16,26] The sphere cluster for* Ec *DHFR is shown in approximately the same orientation as the structure in panel A. In contrast, the sphere cluster for R67 DHFR is shown sideways, after a 90° rotation along the* y*-axis.*

the two subdomains. This binding mode positions NADPH and DHF in individual sites and orients them so that a hydride can be readily transferred from the A side of NADPH to C6 of the *si* face of the pteridine ring in DHF.[10] Comparing numerous bacterial DHFRs, conserved active-site residues include M20, P21, W22, D27, F31, R44, R57, G95, G96, and T113.[11] Other residues are conserved and might play roles in protein folding and/or motion coupled to catalysis.[2,11,12] Movement of a floppy loop (M20 loop) as well as subdomain rotation appear important in minimizing access of solvent to the active site as well as modulating ligand specificity.

Liz Howell received her BS in Chemistry from Muhlenberg College, Allentown, PA, in 1973 and her PhD degree in Chemistry from Lehigh University, Bethlehem, PA, in 1982. She began her dihydrofolate reductase experiences as a postdoctoral researcher with John Abelson and Joe Kraut at the Agouron Institute in San Diego, California, where she constructed and characterized several site-directed mutants of chromosomal E. coli *dihydrofolate reductase (DHFR). She ventured out further on a limb by selecting and studying second site revertants of the D27S lesion. She joined the faculty in the Biochemistry department at the University of Tennessee in 1988 and became a full professor in 2001. She has been studying the R-plasmid encoded R67 DHFR since the early 1990s and been fascinated trying to understand how this enzyme works.*

In contrast, R67 DHFR is a homotetramer possessing a single active-site pore. The presence of only one active site per multimer is quite unusual. Other examples of one binding site per oligomer include the AIDS protease[13] and the central pore in hemoglobin, where 1,3-bisphosphoglycerate binds.[14] Each monomer in R67 DHFR is composed of five antiparallel β-strands.[15,16] This fold has subsequently been identified as occurring in SH3 domains.[17] Three strands from one monomer associate with similar strands from the second monomer, forming a six-stranded β-barrel at the dimer interface. A dimer of dimers involving loop–loop contacts generates the tetramer. The active tetrameric species is toroidal, with the hole being the active site. A 222-symmetry operator occurs at the center of the active-site pore, dictating that for each ligand-binding site there must be three symmetry-related sites arising from 180° rotations along the *x*-, *y*-, or z-axis. The symmetry can be clearly seen in the reverse image of the active site given in Figure 1D. A constriction near the center of the pore occurs, pre-

sumably limiting access to solvent during the hydride-transfer reaction.

These two DHFR structures illustrate totally different topologies. The *Ec* DHFR scaffold contains a specific binding site for the cofactor as well as a specific site for the substrate; the overall structure and binding site are asymmetric. This is the typical situation for most proteins. In contrast, the single active site of R67 DHFR possesses a 222-symmetry operator, which dictates that ligands must share overlapping sites.

3. Ligand Binding

3.1. *E. coli* chromosomal DHFR

The structures of substrate and cofactor are shown in Scheme 1. *Ec* DHFR binds a single molecule of DHF in a predominately hydrophobic binding pocket. The nicotinamide ring of the cofactor is disordered in the DHFR·$NADP^+$ binary complex and becomes ordered in the ternary DHFR·folate·$NADP^+$ state. Binding involves numerous protein–ligand contacts, and specific interactions are listed in refs. [8, 18–20]. Chromosomal DHFR binds its ligands with a large enthalpic component through specific interactions.

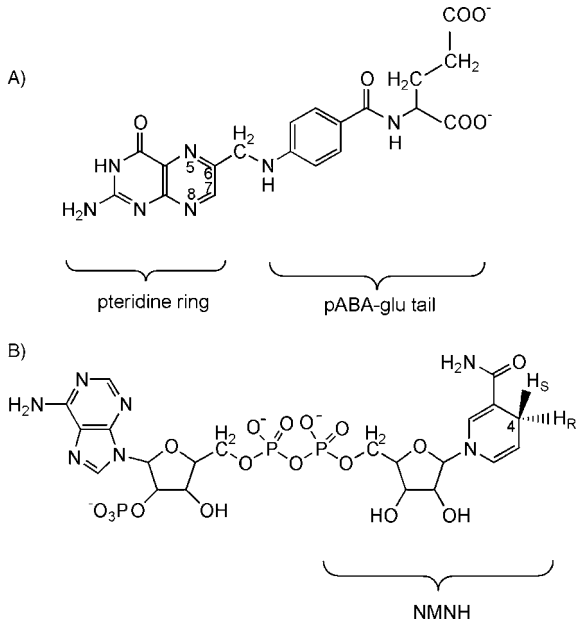

Scheme 1. *The structures of A) folate and B) NADPH. Reduction of folate across the C7–N8 bond yields dihydrofolate while reduction of the N5–C6 double bond produces THF. During catalysis, the A or* re *hydrogen (H_R) on C4 of the nicotinamide ring faces the* si *face of the dihydrofolate pteridine ring, which accepts a hydride at C6. The* pABA-Glu *and NMNH fragments are labeled.*

In *Ec* DHFR, addition of either ligand, followed by the second ligand, leads to formation of the productive ternary complex *Ec* DHFR·NADPH·DHF. After protonation and hydride transfer, products are released in a preferred order with $NADP^+$ leaving first. Subsequent NADPH addition generates the DHFR·THF·NADPH complex. Release of THF occurs next and is the rate-determining step. The resulting DHFR·NADPH complex then binds DHF to initiate a new round of catalysis. Scheme 2 depicts the catalytic steps and their respective rate constants.[21] The differential effects of oxidized/reduced cofactor on THF release indicate some level of interligand cooperativity. Bystroff and Kraut[9] propose that the greatest degree of cooperativity occurs in the transition state and arises from domain as well as floppy-loop movements.

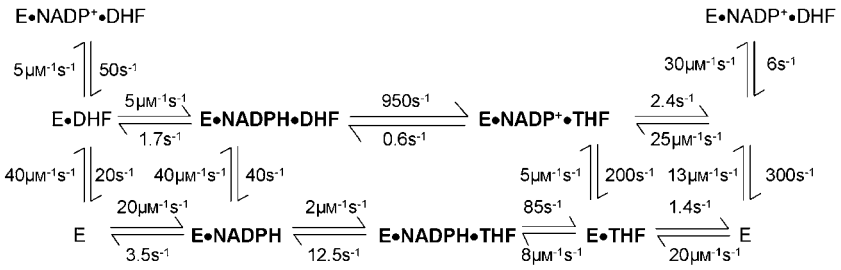

Scheme 2. *The proposed mechanism for* Ec *chromosomal DHFR.[21] Rates were monitored by stopped flow at 25 °C and the values describe pH-independent catalysis. While the initial addition of either substrate or cofactor to free enzyme is random, once the ternary complex is formed, the enzyme follows a preferred pathway, as shown in bold.*

Numerous co-crystal structures of *Ec* chromosomal DHFR (>45) have been obtained, and a comparison suggests substantial movement of the protein, particularly the Met20 loop, is associated with ligand binding as well as catalysis.[20] This loop assumes either an open, closed, or occluded conformation, depending on which ligand(s) are bound. NMR studies of the Met20-loop motion show an oscillation frequency of 35 s^{-1}.[22] That this rate is similar to the release rate for THF suggests that loop movement might be linked to product release. A movie depicting the *Ec* chromosomal DHFR reaction cycle based on the various structures is available at http://chem-faculty.ucsd.edu/kraut/dhfr.html.

3.2. R67 DHFR

Binding studies by time-resolved fluorescence anisotropy as well as isothermal titration calorimetry (ITC) demonstrate that a total of two ligands bind to R67 DHFR. The combinations are two folate (or DHF) molecules, two NADPH molecules, or one NADPH plus one folate/DHF.[23] The first two complexes are nonproductive, while the last one yields products. Binding of two NADPH molecules shows negative cooperativity, which suggests that the first molecule binds at or near the center of symmetry and impedes binding of a second molecule at a symmetry-related site. Binding of two folate molecules shows positive cooperativity, consistent with interactions between the bound folate molecules that enhance affinity. Binding of folate to a 1:1 R67 DHFR·NADPH complex also shows positive cooperativity between NADPH and folate. These various observations support a preferred binding pathway that results in catalysis as shown in Scheme 3. Interligand NOE (ILOE) data

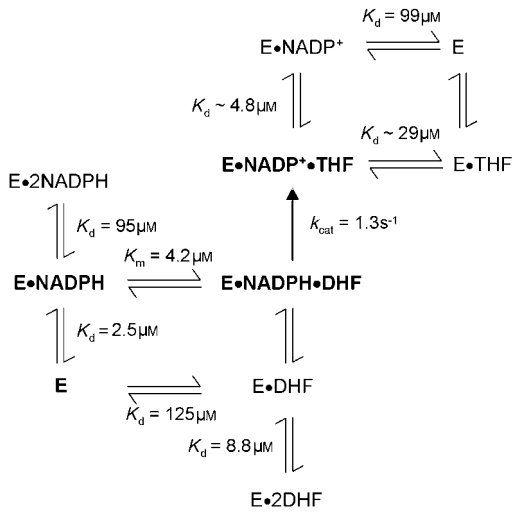

Scheme 3. *The proposed binding mechanism for R67 DHFR.[23] K_d values were monitored by ITC at pH 8.0; kinetic values were obtained from steady-state rates at pH 7.0. The preferred binding pathway is shown in bold.*

from NMR experiments[24] indicate few ILOEs between bound $NADP^+$ and folate; this suggests the ligands are bound in extended conformations on opposite sides and meet somewhere in the middle of the pore.

A cocrystal with two bound folate molecules has been obtained for R67 DHFR (1VIF).[16] Few changes are observed in the protein upon folate binding. If one ligand is bound, there is an equal probability that it will bind to any one of the four equivalent sites within the pore; this effectively dilutes the observed electron density to an average over these four states. Thus, difference maps for bound folate show low density in the pore, representing a composite of overlapping density from two folate molecules bound in two asymmetric sites, each at one-quarter occupancy. Fol I is bound productively with its *si* face exposed, whereas Fol II has its *si* face nestled against the side of the pore, making it unavailable to receive a hydride. Density for the *p*-aminobenzoyl acid-Glu (pABA-Glu) tail was not observed; this is consistent with disorder.

Recent NMR studies have assigned the chemical shifts of backbone and most side-chain residues in R67 DHFR.[25] Measurements of the dynamic behavior of the protein found it to be well-structured and not to display much backbone motion. Internal motions are described in terms of an order parameter, $\langle S^2 \rangle$, which varies between 1 (no internal motion) and 0.[7] Addition of $NADP^+$ to R67 DHFR did not result in any large change in the overall motion of the protein, as $\langle S^2 \rangle$ did not change much ($\langle S^2_{apo} \rangle = 0.89$ versus $\langle S^2_{bound} \rangle = 0.86$); this indicated no to limited motion upon cofactor binding.

Obtaining either a crystal or NMR structure of the ternary complex has proven especially difficult, as the fourfold symmetry within the pore results in a fourfold dilution of the signal. This difficulty, combined with the possibility of binding either folate or NADPH in each site further reduces the signal. Therefore, a computational approach was used to model the productive ternary complex.[26] The bound pteridine ring of Fol I from the crystal structure was used to dock the nicotinamide-ribose-P_i (NMNH) moiety of NADPH. NMNH was positioned by two different algorithms (DOCK and SLIDE),[27,28] on the opposite side of the pore from Fol I, where it interacts with Fol I at the pore's center. The two different docking algorithms yielded similar results for the top-scoring NMNH dockings; this gave confidence in the model. Numerous residues serve dual roles in binding. For example, Q67 from both the B and D subunits has several contacts with the pteridine ring, while the same residue from the A and C subunits has several contacts with the nicotinamide ring. Other residues proposed to be involved in binding both ligands are I68 and Y69. These residues are generally amphipathic, allowing them to make both hydrophobic and hydrophilic contacts with the ligands. The result is a promiscuous binding surface where active-site residues can co-optimize the binding of two ligands and orient them for catalysis.

To obtain further information on the positioning of the pABA-glu tail of folate, which is disordered in the crystal structure, Fol I was removed from the top-scoring R67 DHFR Fol I·NMNH ternary complex and the full-length folate molecule docked. While the pteridine ring of folate docked in the same general position as Fol I, the position of the pABA-Glu tail of folate varied. NADPH was also docked into R67 DHFR·Fol I, and one molecule met the NMR constraints (i.e., *syn* nicotinamide ring with respect to its ribose ring and *anti* adenine ring with respect to its ribose).[24,29] This ternary complex model is depicted in Figure 2. Stacking between the nicotinamide ring of cofactor and the pteridine ring of folate is predicted in this model, consistent with ILOE constraints.[24]

Binding promiscuity in R67 DHFR is also supported by the observation that it can utilize α-NADPH as cofactor[30] as well as be inhibited by novobiocin ($K_i = 70$ μM) and congo red ($K_i = 2$ μM). Neither of the last two ligands resembles NADPH or folate.

The above comparison illustrates that binding of ligands in *Ec* DHFR relies on specific protein contacts. A linkage between catalysis and protein movement has been uncovered, with domain and floppy-loop movement facilitating both binding and catalysis. In contrast, R67 DHFR uses a promiscuous binding surface that accommodates both NADPH and DHF as well as alternate ligands, by using a range of interaction types generated by the presence of amphipathic residues. Interligand cooperativity patterns are particularly important in R67 DHFR.

4. Site-Directed Mutants

4.1. *E. coli* chromosomal DHFR

Numerous mutations have been constructed and evaluated in *Ec* chromosomal DHFR (see refs. [4, 31–33] and references therein). In general, mutations in the DHF-binding pocket affect DHF K_d values over a wide range (1700–0.5-fold), while K_d values for NADPH are concurrently altered to a much smaller degree (3.3–0.45-fold).[4] The general trend observed in these mutants is that DHF, but not NADPH, binding is affected. A similar trend is observed for mutations in the NADPH-bind-

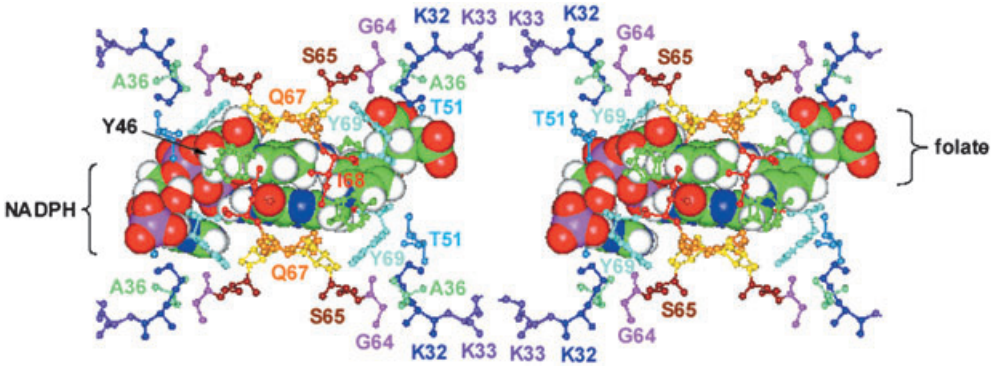

Figure 2. *A stereo view of the R67 DHFR·NADPH·folate complex predicted by DOCK.[26] This image is related to the orientation in Figure 1B by a 90° rotation along the y-axis. This model is consistent with interligand NOEs derived from NMR experiments as well as the A-side stereochemistry of the reaction.[24,29,34,97] The top scoring folate conformer is shown at the top right using a CPK surface. Docked NADPH is depicted at bottom left. For the ligands, the color code is as follows: carbon, green; nitrogen, blue; oxygen, red; phosphorus, magenta; and hydrogen, white. Numerous active site residues in R67 DHFR are shown using ball and stick representations and color-coded labels are provided. Val66 residues (yellow) are unlabeled. Since Ile68 (red) and Tyr46 (green) residues occur on the side of the active site, two of these side chains can be seen near the side of the ligands, while two symmetry-related residues are hidden behind the ligands.*

ing pocket with up to 23-fold increases for NADPH K_d values, while DHF K_d values are only altered up to fourfold. These results indicate that the effects of the mutations are mostly local and focus on the ligand whose contacts are disrupted. Lesser or no effects are observed on binding of the second ligand. Mutations at only one residue, D27, in *Ec* chromosomal DHFR profoundly affect the hydride transfer rate ($>$100-fold).[31]

4.2. R67 DHFR

Single mutations in the R67 DHFR gene result in four mutations per homotetramer. Since R67 DHFR possesses a single active-site pore, the effect of four concurrent mutations on ligand binding can be profound. For example, the cumulative effect of four mutations at either K32, W38, S59, or H62 at the dimer–dimer interfaces results in destabilization of the tetramer such that only dimers are formed.[34–37] A corollary of four mutations occurring simultaneously per active site pore is that mutations most likely need to be conservative to not have very profound effects on protein structure and/or function.

The "one site fits both" model of binding in R67 DHFR predicts that binding to both ligands should be affected by each mutation. This behavior is indeed observed, for example, a Y69F mutant displays tenfold *weaker* binding to DHF and 19-fold *weaker* binding to NADPH than wild-type (wt) R67 DHFR.[38] Also, a Q67H mutant displays 36- and 110-fold *tighter* binding to DHF and NADPH, respectively.[39] In the context of these K_m changes, which vary by up to three orders of magnitude, the ability of the mutations to preferentially alter NADPH versus DHF binding appears marginal. In other words, the Q67H mutant *enhances* NADPH binding (compared to DHF) by only threefold, while the Y69F mutant *weakens* NADPH binding (compared to DHF) by twofold.

While the Q67H mutation tightens binding, it does not lead to enhanced catalytic efficiency as binding is concurrently tightened at all symmetry-related sites. This leads to substantial substrate and cofactor inhibition because of formation of the nonproductive DHF·DHF and NADPH·NADPH complexes.[39,40] Therefore a balance between catalysis and inhibition exists, which can be perturbed by mutations.

Mapping of the active-site surface by a mutagenesis approach as well as use of ionic-strength effects have identified K32, Q67, I68, and Y69 as residues in which conservative mutations have large effects on binding and catalysis.[35,38,39,41] These residues form a stripe that establishes the binding and catalytic surface and are highlighted in blue in Figure 3. The surface for symmetry-related K32, Q67, I68, and Y69 residues describes two continuous stripes that run from one edge of the pore to the other. While residues 67–69 would be expected to lie near each other, the contiguous placement of K32 in this stripe supports its importance.

Because of the 222 symmetry of the R67 DHFR structure, it is difficult to produce local effects that can allow dissection of how each residue interacts with the ligands. Breaking the symmetry of R67 DHFR by introduction of asymmetric mutations suggests one role of the symmetry is to provide an avidity or multivalency effect.[40,42,43] Here, once a site is occupied, the proximity of other symmetry-related sites can enhance binding by reduction of the associated entropy and/or by decreasing the dissociation rate.[44–46]

This section illustrates that active-site mutants of *Ec* DHFR mostly have local effects on ligand binding. Exceptions include mutants that might affect correlated protein motion[11,47] as well as second-site suppressor mutations.[48–50] In contrast, mutations in R67 DHFR can display profound effects, arising from the combination of 222 symmetry imposed on a single active-site pore in a homotetrameric scaffold. Typically binding to both NADPH and DHF are affected to similar extents.

5. Catalysis

5.1. *E. coli* chromosomal DHFR

Chromosomal DHFR is proposed to be a well-evolved enzyme with a catalytic efficiency of 0.15.[51] (For comparison, the efficiency for triose phosphate isomerase, which has been de-

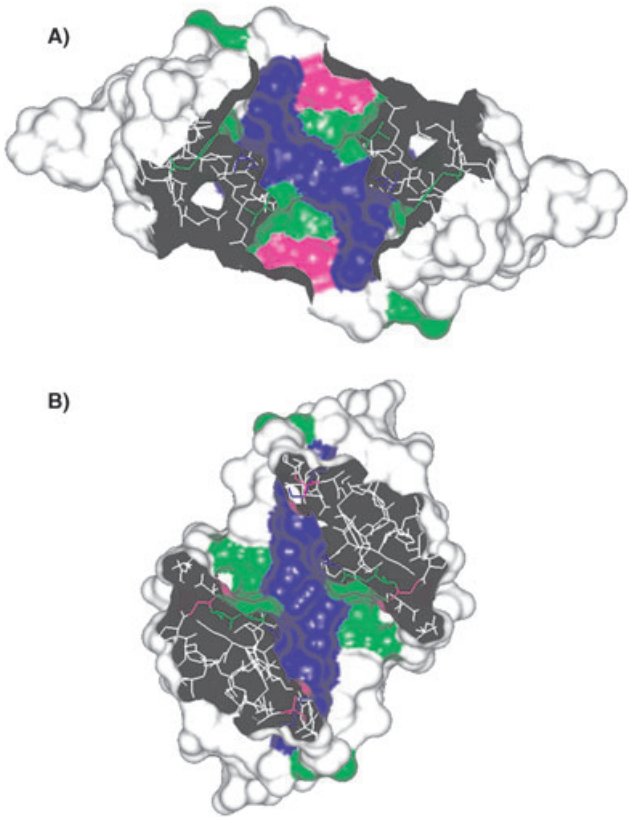

Figure 3. *A map of active site residues identified as important to binding and catalysis in the R67 DHFR reaction.[35,38,39,41] A) Depiction of a single dimer–dimer interface in R67 DHFR by using a Connolly surface. This view is related to Figure 1B by a 90° rotation along the x axis. B) Depiction of a single monomer–monomer interface. This view is related to Figure 1B by a 90° rotation along the y-axis. Residues where conservative mutations displayed a greater than fivefold effect are colored blue (K32, Q67, I68, Y69). Residues where conservative mutations displayed no to minimal effects are colored green (K33, Y46, T51, S65, V66). Residues where mutations apparently perturbed the quaternary/tertiary structure are colored magenta (A36, G64).*

scribed as a "perfect enzyme," is 0.6.)[52] A conserved acidic group (Asp in bacterial DHFRs and Glu in mammalian DHFRs) has been proposed to facilitate catalysis, although the exact mechanism remains debated. Characterization of a D27S *Ec* DHFR mutant shows a 70-fold decrease in k_{cat} and a 50-fold increase in K_m.[31] However, k_{cat} in this mutant increased as the pH was decreased, consistent with the increased availability of preprotonated, activated DHF (N5 pK_a = 2.59).[53] More recent resonance Raman studies on the wt and D27S enzymes suggest this aspartate acts by raising the N5 pK_a of DHF to 6.5.[54,55] This scenario is supported by a recent computational study.[56] Alternatively, another computational study suggests D27 uses an electrostatic mechanism to facilitate enol tautomer formation in DHF.[57] Another scenario arises from NMR studies with the *Lactobacillus casei* DHFR, which show that the analogous D26 remains ionized in all complexes studied.[58] This group proposes that aspartate polarizes bound DHF. Finally, Cummins and Gready propose direct donation of the proton to N5 (a keto cation) without the necessity of an enol intermediate.[59]

Movement of the Met20 floppy-loop sequesters the hydride-transfer event from solvent. The exact sequence of protonation donation and hydride transfer is not clear in *Ec* chromosomal DHFR. A combination of solvent and NADPD isotope effects support protonation prior to hydride transfer.[60] More recent molecular-dynamics (MD) calculations propose the reverse sequence.[61]

Other factors have been proposed to facilitate catalysis. A positive electrostatic potential around the active site of *Ec* DHFR might steer binding of the negatively charged substrate and cofactor.[62] Ab initio quantum-mechanical calculations suggest that polarization of bound substrate and cofactor occur upon binding and serve to facilitate hydride transfer.[63–66]

More recently, motion of the protein chain, including subdomain rotation and alternate active-site loop conformations, has been proposed to modulate ligand specificity and catalytic efficiency.[3,11,47,67,68] This model invokes "promoting protein motion" as a means to enhance crossing the reaction barrier, ultimately enhancing the catalytic rate. Conserved amino acids distant from the active site, mixed quantum/classical MD calculations, site-directed-mutagenesis studies, and NMR experiments are all considered in invoking this hypothesis. The involvement of distant residues in catalysis is also supported by the identification of second-site suppressor mutations of the D27S lesion. These suppressing mutations include F137S, F153S, or I155N, and their presence in the D27S context enhances catalytic efficiency two- to threefold. Unexpectedly, all three residues occur on the surface of the protein and are approximately 15, 8, and 14 Å distant from the D27 residue in the active site, respectively.[48–50] Most recently, reports indicate that *Ec* DHFR uses tunneling in its reaction.[69,70]

5.2. R67 DHFR

Given the configuration of its active-site, it is unlikely that R67 DHFR has been able to acquire a residue similar to D27 in *Ec* chromosomal DHFR. This limitation occurs because addition of a single mutation (in the gene) that might activate DHF will result in four mutations per active site. While addition of a general acid might activate DHF in one site, it would more than likely impede NADPH binding in the other symmetry-related site(s). To identify any potential groups involved in catalysis, the pH profile of a H62C R67 DHFR was monitored.[34] This mutant stabilized the active tetramer from pH 4–9 by disulfide-bond formation. Its pH profile resembled that of the *Ec* D27S DHFR mutant, with increasing activity as the pH was lowered. This behavior is consistent with the use of protonated DHF as the productive substrate and no contributions from acidic groups in the enzyme. Raman difference measurements also show no indication of bound protonated DHF at pH 5.3; this suggests that the active site environment of R67 DHFR does not greatly alter the pK_a of N5 in DHF from the solution value of 2.59.[71] This observation is consistent with the active site's being large and accessible to solvent.

Interligand interactions appear quite important to the R67 DHFR reaction. Various pairs of ligands compete for binding to the active-site pore with the DHF·DHF and NADPH·NADPH

complexes being nonproductive. From both crystallography and NMR studies, the 2DHF/folate molecules stack near the center of the pore[16,24] in a manner perhaps similar to their solution dimeric structure.[72] From docking studies as well as monitoring interligand NOEs, the folate·$NADP^+$ complex also appears to involve stacking between the nicotinamide and pteridine rings. Thus, ring stacking might be strongly correlated with the positive cooperativity associated with 2DHF/folate and NADPH·folate complex formation. Does R67 DHFR also play a role in this cooperativity? From studies of asymmetric Q67H mutants, Q67 at the center of the pore helps discriminate between the various complexes, with a strong preference for the productive NADPH·DHF pair.[40] This result suggests that an interplay between the wt protein and the interligand complexes provides a funnel towards transition-state formation.

When ternary-complex formation is studied by ITC, the ΔH value associated with addition of folate to wt and mutant R67 DHFR·NADPH complexes shows a potential linear correlation with catalytic efficiency (Figure 4). Previous linear free-energy

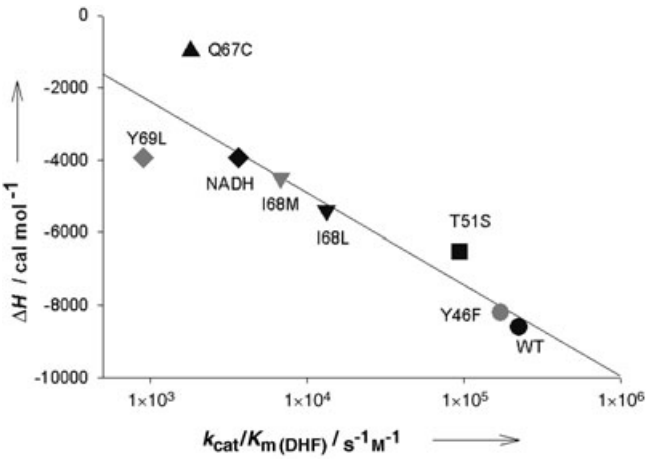

Figure 4. *A potential linear correlation between the heat of enthalpy for binding of folate to R67 DHFR·NADPH (pH 8) and log k_{cat}/K_m (pH 7).[41] The binding enthalpy was monitored by ITC upon addition of the poor substrate, folate, to the R67 DHFR·NADPH complex.[23] wt R67 DHFR data are given by ●, Y46F by ○, T51S by ■, I68L by ▼, I68M by ▽, NADH by ◆, Y69L by ◇, and Q67C by ▲ points. A similar correlation was also noted for the $k_{cat}/K_{m\,(NADPH)}$ data. Reduction of folate is minimal under these conditions as its k_{cat} is quite low at pH 8 and the titrations were done at 13 °C. Additional controls indicate that any contribution of catalysis to the binding curves are minimal.[23,41]*

relationships have been observed and have been proposed to describe the necessary interplay between binding energy and catalysis.[73–75] From NMR studies of vancomycin dimerization, structural tightness (i.e. close contact and increased rigidity) appears to display a positive correlation with the enthalpy (e.g. exothermicity) of the binding interaction.[76–78] Therefore, these R67 DHFR results support the hypothesis that interligand interactions play a strong role in binding as well as catalysis. These experimental data are consistent with the docked ternary-complex model shown in Figure 2 and predict stacking between NADPH and folate. As mutations are introduced, a caveat is that the orientation between ligands remains suitable for hydride transfer. Use of the alternate cofactor, NADH (◆ point in Figure 4), extends this correlation and suggests that looseness of binding (derived either from alternate ligands or protein mutations) controls catalytic efficiency. Our studies also support recent reports suggesting a strong role for enthalpy associated with catalytic function.[79–83]

Electrostatics also appear to be important in R67 DHFR catalysis as the active-site pore is predicted, by solving a nonlinear Poisson–Boltzman equation, to be positively charged.[26] Residues implicated in establishing the positive potential are K32 and K33. Salt effects on NADPH binding uncovered two ionic interactions with R67 DHFR.[35] (Quantitation of salt effects by plots of log K_d versus log (ionic strength) have previously been taken to describe Z, the number of ionic interactions involved in binding.[84,85]) When R67 DHFR's steady-state kinetic behavior was probed by increasing salt concentrations, at least one ionic interaction was identified in binding NADPH (K_m effects). An unusual enhancement of k_{cat} by increasing salt concentrations was noted, consistent with breaking of a salt bridge that allowed the ground state to move towards the transition state. The resulting model for catalysis invokes tight binding of NADPH through ionic interactions between two, symmetry-related K32 residues (located on different monomers at one end of the pore) with the 2′-phosphate and pyrophosphate groups. Loss of an ionic interaction between a symmetry-related K32 residue in the second half of the pore with the Glu tail of DHF might be the key event that facilitates catalysis.[42] This scenario could permit the ligands to move towards a position associated with the correct distance and angle for hydride transfer as well as to exclude solvent. This unusual mechanism likely arises from the need to balance catalysis with the constraints imposed by the 222 symmetry of the active site pore.

Finally, NMR studies reveal that $NADP^+$ binds to R67 DHFR with a *syn* relationship between the nicotinamide ring with its ribose (i.e., the carboxamide group from the nicotinamide and the ribose ring oxygen atom are close.)[24,29] When this observation is coupled with the experimentally determined A-side hydride-transfer reaction, a *syn* periplanar orientation during R67 DHFR catalysis is predicted. (If the reduced nicotinamide ring is in a quasi-boat geometry, the relation between the antibonding orbital of the ribose-ring oxygen atom with the unshared electrons on N4 of the nicotinamide ring can be either periplanar or antiperiplanar (see ref. [86] and references therein). Since the vast majority of reductases utilize either the *anti* antiperiplanar configuration for A-side transfer or the *syn* antiperiplanar conformation for B-side transfer, this topology in R67 DHFR is quite unusual.

The above evidence supports the contention that *Ec* chromosomal DHFR is a well-evolved enzyme, orchestrating various components to facilitate catalysis, including its conserved Asp27 residue to activate bound DHF, electrostatics and possibly protein motion as well as tunneling. In contrast, R67 DHFR appears simpler in its approach. Its rate-determining step is chemistry, the active site is solvent-accessible except perhaps at the hourglass center, no amino acid (such as D27) is present, and preprotonated DHF from solution is used as substrate. The ability to discriminate between the homoligand and hetero-

ligand complexes appears to mostly arise from stacking between the ligands, as well as some contribution from the enzyme. For the productive ternary complex, the greater the enthalpy associated with complex formation (i.e. structural tightness), the greater the catalytic efficiency.

6. Transition States?

At least two different transition states are available to the DHFR reaction,[87] as illustrated in Figure 5. Constraints imposed by the *Ec* chromosomal DHFR structure lead to its using an *exo* transition state with minimal overlap of the pteridine and nicotinamide rings.[88] In this model, the pteridine and nicotinamide rings approach edge-on. In contrast, interligand-NOE NMR data favor R67 DHFR's using an *endo* transition state[24] as does the docked ternary-complex model.[26] The *endo* transition state positions the nicotinamide ring over the more bulky side of the pteridine ring. (An *endo*-type geometry has also been identified in the pteridine reductase structure (1E92 in the PDB). This enzyme is a short-chain dehydrogenase from *Leishmania* and *Trypanosoma* that displays partial stacking of the nicotinamide and pterin ring systems.[89]) Quantum-mechanical calculations evaluate the *endo* transition state as being 2–8 kcal mol^{-1} more stable than the *exo* transition state because of the interring interactions.[87,88] The importance of interligand interactions in R67 DHFR catalysis is no surprise; this modality plays an essential role in discriminating between the various two ligand complexes.

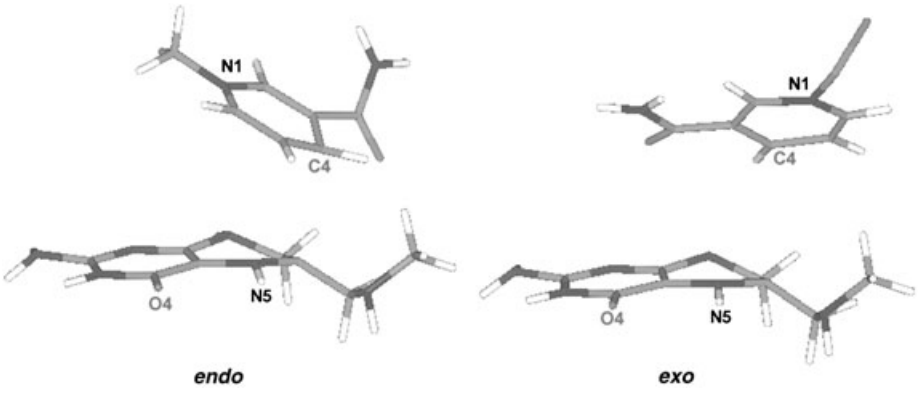

Figure 5. *Two transition-state conformations for the DHFR reaction.[87,88] Coordinates for these models were kindly provided by Luis Domingo.[87] The pteridine rings lie on the bottom of the image; the N5 atoms are labeled and pointing towards the viewer. The nicotinamide rings occur at the top of the image; their C4 atoms are labeled.*

Can primary isotope effects allow differentiation between the two transition states? Experimentally, the measured kinetic isotope effects appear similar, as NADPD isotope effects with a H62C mutant of R67 DHFR find ^{D}V ($=k_{cat}$ on using NADPH/k_{cat} on using NADPD) at pH 5.0 to equal 3.6 ± 0.45 and $^{D}V=3.3\pm0.33$ at pH 7.0.[34] These results indicate that hydride transfer is fully rate-determining from pH 5–7. These values are similar to those measured for *Ec* chromosomal DHFR by monitoring steady-state kinetics at pH 9, at which hydride transfer is rate limiting ($^{D}V=2.7\pm0.3$[90]). Additional stopped-flow experiments with *Ec* DHFR monitored its hydride-transfer rate directly at pH 7 and found a kinetic isotope effect of 3.0 ± 0.1 at 25 °C.[21] Most recently, Sikorski et al., by a combination of primary and secondary isotope effects, calculated the intrinsic isotope effect of *Ec* DHFR as 3.5 ± 0.2 at 25 °C.[70]

Given all the limitations imposed by the 222 symmetry, how can R67 DHFR work as well as it does? Most likely, use of the more stable transition state allows catalysis to occur. This comparison also points towards independent evolutionary pathways for the *Ec* and R67 DHFRs, this time involving the transition state of the reaction.

7. Conclusions and Perspectives

A general hypothesis in enzymology is that increasing levels of preorganization in an enzyme active site lead to enhanced catalytic efficiency.[3,91,92] *Ec* chromosomal DHFR clearly does this by binding its ligands in well-defined pockets. Juxtaposed binding sites allow the ligands to be oriented such that hydride transfer is readily achieved. Protein movement includes floppy (M20) loop movement to limit access of bulk solvent to the active site as well as protein motion that might funnel energy to the active site and aid barrier-crossing events. These proposals all suggest chromosomal *Ec* DHFR has developed numerous strategies to maximize catalytic efficiency.

In contrast to the above devices, R67 DHFR has developed an alternate path to catalysis. The initial binding of NADPH utilizes the symmetry of the protein by allowing binding to one of four symmetry-related sites. Once bound, NADPH creates a local asymmetric environment in the active-site pore that results in negative cooperativity disfavoring binding of a second NADPH molecule or positive cooperativity favoring binding of DHF. Both these cooperativity patterns favor channeling of the binding pathway towards the productive ternary complex, NADPH·DHF. These observations suggest that some level of "preorganization" arises by generation of asymmetry upon binding the first ligand.[93–96] A corollary of this model is that ligand–ligand cooperativity plays an important role in catalysis. Inextricably coupled to the 222 symmetry is the use of a "one site fits both" approach as well as the inability of the enzyme to accumulate mutations without strongly affecting either protein stability, oligomerization state or binding and catalysis.

From an "enzyme's eye view", what is important to DHFR catalysis can be gleaned by what is similar in these two approaches to DHF reduction. These features are: 1) use of a positive electrostatic potential to guide the negatively charged ligands to the active sites, 2) once DHF is bound, use of Asp27 in *Ec* DHFR to activate substrate or a proton from solution in

R67 DHFR (and D27S *Ec* DHFR), and 3) the proximity of the catalytic atoms, although directed by different guiding principles. For *Ec* DHFR, the reaction is driven by protein–ligand interactions to result in juxtaposed sites that compress the distance between C6 of DHF and C4 of the nicotinamide ring, while in R67 DHFR, the reaction appears to have a significant component supplied by interligand cooperativity.

Given these widely different structures and strategies, it is remarkable that the hydride-transfer rate for the primitive R67 enzyme is only ~180-fold less than that for the well-evolved enzyme, *Ec* DHFR (see Table 1). Further, the D27S mutant in *Ec* DHFR possesses a lower k_{cat} (threefold) and a much lower efficiency ($k_{cat}/K_{m\,(DHF)}$) than R67 DHFR (30-fold; see ref. [49] and Table 1). This convergence suggests that the level of DHFR activity that is possible without catalytic machinery (e.g. general acids, bases) has a finite range. It is particularly surprising that R67 DHFR is more efficient than the D27S *Ec* DHFR given all the additional mechanisms proposed for promoting *Ec* DHFR function (tunneling, overlapping binding sites for substrate and cofactor, "promoting protein motion", etc). Thus, R67 DHFR might provide additional surprises concerning its contributions towards catalysis.

Abbreviations

DHF, dihydrofolate; *Ec* DHFR, *E. coli* chromosomal dihydrofolate reductase; Fol 1 and Fol 2, the pteridine rings of two folates in the 1VIF crystal structure; NADP(+/H), nicotinamide adenine dinucleotide phosphate (oxidized/reduced form); ILOE, interligand nuclear Overhauser effect; ITC, isothermal titration calorimetry; μ, ionic strength; NMNH, the reduced nicotinamide-ribose-P_i moiety of NADPH; pABA-Glu, *p*-aminobenzoylglutamic acid tail of DHF; R67 DHFR, R67 dihydrofolate reductase; THF, tetrahydrofolate; TMP, trimethoprim; wt, wild type.

Mutants are described by the wt residue and numbered position in the sequence, followed by the amino acid substitution. For example, Q67H R67 DHFR describes the Gln67→His mutation. For brevity, when a single residue in R67 DHFR is mentioned in the text, all four symmetry equivalent residues are implied.

Acknowledgements

Without all the efforts of present and past lab members, this review would not have been possible. I particularly thank Derike Smiley for proposing the idea of this review and Cynthia Peterson for her helpful comments on the text. This research was supported by NSF grant MCB-0131394.

Keywords: antibiotics · enthalpy · enzyme catalysis · enzyme evolution · protein engineering

[1] P. A. White, W. D. Rawlinson, *J. Antimicrob. Chemother.* **2001**, *47*, 495–496.
[2] S. J. Benkovic, S. Hammes-Schiffer, *Science* **2003**, *301*, 1196–1202.
[3] P. T. Rajagopalan, S. J. Benkovic, *Chem. Rec.* **2002**, *2*, 24–36.
[4] G. P. Miller, S. J. Benkovic, *Chem. Biol.* **1998**, *5*, R105–113.
[5] K. A. Brown, J. Kraut, *Faraday Discuss.* **1992**, 217–224.
[6] J. Feeney, *Angew. Chem.* **2000**, *112*, 298–321; *Angew. Chem. Int. Ed.* **2000**, *39*, 290–312.
[7] J. R. Schnell, H. J. Dyson, P. E. Wright, *Annu. Rev. Biophys. Biomol. Struct.* **2004**, *33*, 119–140.
[8] J. Bolin, D. Filman, D. Matthews, R. Hamlin, J. Kraut, *J. Biol. Chem.* **1982**, *257*, 13650–13662.
[9] C. Bystroff, J. Kraut, *Biochemistry* **1991**, *30*, 2227–2239.
[10] E. J. Pastore, M. Friedkin, *J. Biol. Chem.* **1962**, *237*, 3802–3810.
[11] P. K. Agarwal, S. R. Billeter, P. T. Rajagopalan, S. J. Benkovic, S. Hammes-Schiffer, *Proc. Natl. Acad. Sci. USA* **2002**, *99*, 2794–2799.
[12] M. Iwakura, T. Nakamura, C. Yamane, K. Maki, *Nat. Struct. Biol.* **2000**, *7*, 580–585.
[13] A. Wlodawer, M. Miller, M. Jaskolshki, B. K. Sathyanarayana, E. Baldwin, I. T. Weber, L. M. Selk, L. Clawson, J. Schneider, S. B. H. Kent, *Science* **1989**, *245*, 616–621.
[14] A. Arnone, *Nature* **1972**, *247*, 146–147.
[15] D. A. Matthews, S. L. Smith, D. P. Baccanari, J. J. Burchall, S. J. Oatley, J. Kraut, *Biochemistry* **1986**, *25*, 4194–4204.
[16] N. Narayana, D. A. Matthews, E. E. Howell, N. H. Xuong, *Nat. Struct. Biol.* **1995**, *2*, 1018–1025.
[17] T. V. Borchert, M. Mathieu, J. P. Zeelen, S. A. Courtneidge, R. K. Wierenga, *FEBS Lett.* **1994**, *341*, 79–85.
[18] C. Bystroff, S. J. Oatley, J. Kraut, *Biochemistry* **1990**, *29*, 3263–3277.
[19] D. J. Filman, J. T. Bolin, D. A. Matthews, J. Kraut, *J. Biol. Chem.* **1982**, *257*, 13663–13672.
[20] M. R. Sawaya, J. Kraut, *Biochemistry* **1997**, *36*, 586–603.
[21] C. A. Fierke, K. A. Johnson, S. J. Benkovic, *Biochemistry* **1987**, *26*, 4085–4092.
[22] C. J. Falzone, P. E. Wright, S. J. Benkovic, *Biochemistry* **1994**, *33*, 439–442.
[23] T. D. Bradrick, J. M. Beechem, E. E. Howell, *Biochemistry* **1996**, *35*, 11414–11424.
[24] D. Li, L. A. Levy, S. A. Gabel, M. S. Lebetkin, E. F. DeRose, M. J. Wall, E. E. Howell, R. E. London, *Biochemistry* **2001**, *40*, 4242–4252.
[25] W. H. Pitcher, 3rd, E. F. DeRose, G. A. Mueller, E. E. Howell, R. E. London, *Biochemistry* **2003**, *42*, 11150–11160.
[26] E. E. Howell, U. Shukla, S. N. Hicks, R. D. Smiley, L. A. Kuhn, M. I. Zavodszky, *J. Comput.-Aided Mol. Des.* **2001**, *15*, 1035–1052.
[27] B. K. Shoichet, I. D. Kuntz, *Protein Eng.* **1993**, *6*, 723–732.
[28] V. Schnecke, C. A. Swanson, E. D. Getzoff, J. A. Tainer, L. A. Kuhn, *Proteins* **1998**, *33*, 74–87.
[29] R. M. Brito, F. B. Rudolph, P. R. Rosevear, *Biochemistry* **1991**, *30*, 1461–1469.
[30] S. L. Smith, J. J. Burchall, *Proc. Natl. Acad. Sci. USA* **1983**, *80*, 4619–4623.
[31] E. E. Howell, J. E. Villafranca, M. S. Warren, S. J. Oatley, J. Kraut, *Science* **1986**, *231*, 1123–1128.
[32] J. A. Adams, C. A. Fierke, S. J. Benkovic, *Biochemistry* **1991**, *30*, 11046–11054.
[33] C. R. Wagner, S. J. Benkovic, *Trends Biotechnol.* **1990**, *8*, 263–270.
[34] H. Park, P. Zhuang, R. Nichols, E. E. Howell, *J. Biol. Chem.* **1997**, *272*, 2252–2258.
[35] S. N. Hicks, R. D. Smiley, J. B. Hamilton, E. E. Howell, *Biochemistry* **2003**, *42*, 10569–10578.
[36] F. W. West, H. S. Seo, T. D. Bradrick, E. E. Howell, *Biochemistry* **2000**, *39*, 3678–3689.
[37] J. Dam, T. Rose, M. E. Goldberg, A. Blondel, *J. Mol. Biol.* **2000**, *302*, 235–250.
[38] M. B. Strader, R. D. Smiley, L. G. Stinnett, N. C. VerBerkmoes, E. E. Howell, *Biochemistry* **2001**, *40*, 11344–11352.
[39] H. Park, T. D. Bradrick, E. E. Howell, *Protein Eng.* **1997**, *10*, 1415–1424.
[40] R. D. Smiley, L. G. Stinnett, A. M. Saxton, E. E. Howell, *Biochemistry* **2002**, *41*, 15664–15675.
[41] M. B. Strader, S. Chopra, M. Jackson, R. D. Smiley, L. G. Stinnett, J. Wu, E. E. Howell, *Biochemistry* **2004**, *43*, 7403–7412.
[42] S. N. Hicks, R. D. Smiley, L. G. Stinnett, K. H. Minor, E. E. Howell, *J Biol Chem.* **2004**, *279*, 46995–47002.
[43] L. G. Stinnett, R. D. Smiley, S. N. Hicks, E. E. Howell, *J Biol Chem.* **2004**, *279*, 47003–47009.
[44] C. F. Brewer, M. C. Miceli, L. G. Baum, *Curr. Opin. Struct. Biol.* **2002**, *12*, 616–623.

[45] D. S. Goodsell, A. J. Olson, *Annu. Rev. Biophys. Biomol. Struct.* **2000**, *29*, 105 – 153.
[46] P. I. Kitov, D. R. Bundle, *J. Am. Chem. Soc.* **2003**, *125*, 16 271 – 16 284.
[47] P. T. Rajagopalan, S. Lutz, S. J. Benkovic, *Biochemistry* **2002**, *41*, 12 618 – 12 628.
[48] A. Dion, C. E. Linn, T. D. Bradrick, S. Georghiou, E. E. Howell, *Biochemistry* **1993**, *32*, 3479 – 3487.
[49] E. E. Howell, C. Booth, M. Farnum, J. Kraut, M. S. Warren, *Biochemistry* **1990**, *29*, 8561 – 8569.
[50] K. A. Brown, E. E. Howell, J. Kraut, *Proc. Natl. Acad. Sci. USA* **1993**, *90*, 11 753 – 11 756.
[51] C. A. Fierke, R. D. Kuchta, K. A. Johnson, S. J. Benkovic, *Cold Spring Harbor Symp. Quant. Biol.* **1987**, *52*, 631 – 638.
[52] W. J. Albery, J. R. Knowles, *Biochemistry* **1976**, *15*, 5631 – 5640.
[53] G. Maharaj, B. S. Selinsky, J. R. Appleman, M. Perlman, R. E. London, R. L. Blakley, *Biochemistry* **1990**, *29*, 4554 – 4560.
[54] Y. Q. Chen, J. Kraut, R. L. Blakley, R. Callender, *Biochemistry* **1994**, *33*, 7021 – 7026.
[55] H. Deng, R. Callender, *J. Am. Chem. Soc.* **1998**, *120*, 7730 – 7737.
[56] T. H. Rod, C. L. Brooks, 3rd, *J. Am. Chem. Soc.* **2003**, *125*, 8718 – 8719.
[57] W. Cannon, B. Garrison, S. J. Benkovic, *J. Am. Chem. Soc.* **1997**, *119*, 2386 – 2395.
[58] M. G. Casarotto, J. Basran, R. Badii, K. H. Sze, G. C. Roberts, *Biochemistry* **1999**, *38*, 8038 – 8044.
[59] P. L. Cummins, J. E. Gready, *J. Am. Chem. Soc.* **2001**, *123*, 3418 – 3428.
[60] J. Morrison, S. Stone, *Biochemistry* **1988**, *27*, 5499 – 5506.
[61] P. Shrimpton, R. K. Allemann, *Protein Sci.* **2002**, *11*, 1442 – 1451.
[62] J. Bajorath, D. H. Kitson, J. Kraut, A. T. Hagler, *Proteins* **1991**, *11*, 1 – 12.
[63] J. Bajorath, Z. Q. Li, G. Fitzgerald, D. H. Kitson, M. Farnum, R. M. Fine, J. Kraut, A. T. Hagler, *Proteins* **1991**, *11*, 263 – 270.
[64] J. Bajorath, J. Kraut, Z. Q. Li, D. H. Kitson, A. T. Hagler, *Proc. Natl. Acad. Sci. USA* **1991**, *88*, 6423 – 6426.
[65] J. Bajorath, D. H. Kitson, G. Fitzgerald, J. Andzelm, J. Kraut, A. T. Hagler, *Proteins* **1991**, *9*, 217 – 224.
[66] S. P. Greatbanks, J. E. Gready, A. C. Limaye, A. P. Rendell, *Proteins* **1999**, *37*, 157 – 165.
[67] J. Radkiewicz, I. C. Brooks, *J. Am. Chem. Soc.* **2000**, *122*, 225 – 231.
[68] H. Pan, J. C. Lee, V. J. Hilser, *Proc. Natl. Acad. Sci. USA* **2000**, *97*, 12 020 – 12 025.
[69] M. Garcia-Viloca, D. G. Truhlar, J. Gao, *Biochemistry* **2003**, *42*, 13 558 – 13 575.
[70] R. S. Sikorski, L. Wang, K. A. Markham, P. T. R. Rajagopalan, S. J. Benkovic, A. Kohen, *J. Am. Chem. Soc.* **2004**, *126*, 4778 – 4779.
[71] H. Deng, R. Callender, E. E. Howell, *J. Biol. Chem.* **2001**, *276*, 48 956 – 48 960.
[72] M. Poe, *J. Biol. Chem.* **1977**, *252*, 3724 – 3728.
[73] W. P. Jencks, *Adv. Enzymol. Relat. Areas Mol. Biol.* **1975**, *43*, 219 – 410.
[74] J. O. Goldsmith, L. C. Kuo, *J. Biol. Chem.* **1993**, *268*, 18 481 – 18 484.
[75] J. M. Avis, A. R. Fersht, *Biochemistry* **1993**, *32*, 5321 – 5326.
[76] C. T. Calderone, D. H. Williams, *J. Am. Chem. Soc.* **2001**, *123*, 6262 – 6267.
[77] D. H. Williams, E. Stephens, M. Zhou, *J. Mol. Biol.* **2003**, *329*, 389 – 399.
[78] D. H. Williams, E. Stephens, M. Zhou, *Chem. Commun.* **2003**, 1973 – 1976.
[79] T. C. Bruice, S. J. Benkovic, *Biochemistry* **2000**, *39*, 6267 – 6274.
[80] T. C. Bruice, *Acc. Chem. Res.* **2002**, *35*, 139 – 148.
[81] M. J. Snider, S. Gaunitz, C. Ridgway, S. A. Short, R. Wolfenden, *Biochemistry* **2000**, *39*, 9746 – 9753.
[82] R. Wolfenden, M. J. Snider, *Acc. Chem. Res.* **2001**, *34*, 938 – 945.
[83] J. Villa, M. Strajbl, T. M. Glennon, Y. Y. Sham, Z. T. Chu, A. Warshel, *Proc. Natl. Acad. Sci. USA* **2000**, *97*, 11 899 – 11 904.
[84] M. T. Record, Jr., T. M. Lohman, P. De Haseth, *J. Mol. Biol.* **1976**, *107*, 145 – 158.
[85] C. Park, R. T. Raines, *J. Am. Chem. Soc.* **2001**, *123*, 11 472 – 11 479.
[86] O. B. Almarsson, C. Thomas, *J. Am. Chem. Soc.* **1993**, *115*, 2125 – 2138.
[87] J. Andrés, V. Moliner, V. S. Safont, L. R. Domingo, M. T. Picher, J. Krechl, *Bioorg. Chem.* **1996**, *24*, 10 – 18.
[88] R. Castillo, J. Andrés, V. Moliner, *J. Am. Chem. Soc.* **1999**, *121*, 12 140 – 12 147.
[89] D. G. Gourley, A. W. Schuttelkopf, G. A. Leonard, J. Luba, L. W. Hardy, S. M. Beverley, W. N. Hunter, *Nat. Struct. Biol.* **2001**, *8*, 521 – 525.
[90] J. T. Chen, K. Taira, C. P. Tu, S. J. Benkovic, *Biochemistry* **1987**, *26*, 4093 – 4100.
[91] A. Warshel, *J. Biol. Chem.* **1998**, *273*, 27 035 – 27 038.
[92] S. Marti, M. Roca, J. Andrés, V. Moliner, E. Silla, I. Tunon, J. Bertran, *Chem. Soc. Rev.* **2004**, *33*, 98 – 107.
[93] C. R. Bloom, N. C. Kaarsholm, J. Ha, M. F. Dunn, *Biochemistry* **1997**, *36*, 12 759 – 12 765.
[94] P. C. Marijuan, *Biosystems* **1996**, *38*, 163 – 171.
[95] T. L. Blundell, N. Srinivasan, *Proc. Natl. Acad. Sci. USA* **1996**, *93*, 14 243 – 14 248.
[96] I. Stewart, M. Golubitsky, *Fearful Symmetry: Is God a Geometer?* Blackwell, Cambridge, MA, **1992**.
[97] R. M. Brito, R. Reddick, G. N. Bennett, F. B. Rudolph, P. R. Rosevear, *Biochemistry* **1990**, *29*, 9825 – 9831.
[98] J. Liang, H. Edelsbrunner, C. Woodward, *Protein Sci.* **1998**, *7*, 1884 – 1897.
[99] S. R. Stone, J. F. Morrison, *Biochim. Biophys. Acta* **1986**, *869*, 275 – 285.
[100] S. G. Amyes, J. T. Smith, *Eur. J. Biochem.* **1976**, *61*, 597 – 603.
[101] L. J. Reece, R. Nichols, R. C. Ogden, E. E. Howell, *Biochemistry* **1991**, *30*, 10 895 – 10 904.

Received: July 9, 2004

